Supplemental Material (not copyedited or formatted) for: Sébastien Lion, Mike Boots, Akira Sasaki. 2022. "Multimorph Eco-Evolutionary Dynamics in Structured Populations." The American Naturalist 200(3). DOI: https://doi.org/10.1086/720439.

Online Supplement:

Multi-morph eco-evolutionary dynamics in structured populations

Sébastien Lion[1,*], Mike Boots[3,4] and Akira Sasaki[4,5]

1. CEFE, CNRS, Univ Montpellier, EPHE, IRD, Univ Paul Valéry Montpellier 3. 1919, route de Mende, Montpellier, France.

Email: sebastien.lion@cefe.cnrs.fr. ORCID: 0000-0002-4081-0038.

2. Integrative Biology, University of California, Berkeley, USA. CA 94720.

Email: mboots@berkeley.edu. ORCID: 0000-0003-3763-6136.

3. Biosciences, University of Exeter, Penryn Campus, UK. TR10 9FE.

4. Department of Evolutionary Studies of Biosystems, The Graduate University of Advanced Studies, SOKENDAI, Hayama, Kanagawa 2400139, Japan.

Email: sasaki_akira@soken.ac.jp. ORCID: 0000-0003-3582-5865.

5 Evolution and Ecology Program, International Institute for Applied Systems Analysis, Schlosplatz 1, A-2361, Laxenburg, Austria.

* corresponding author

S1 Justification of equality (A.4)

To justify equation (A.4), we first start from the natural assumption that individuals with the same phenotypes have the same per-capita growth rate in each class (say k) whichever morph they belong:

$$\frac{\mathrm{d}\ln(f_i^k(t)\phi_i^k(z,t))}{\mathrm{d}t} = \frac{\mathrm{d}\ln(\phi^k(z,t))}{\mathrm{d}t}$$

This is equation (A.2) in Appendix A. We write the same relationship in class j:

$$\frac{\mathrm{d}\ln(f_i^j(t)\phi_i^j(z,t)}{\mathrm{d}t} = \frac{\mathrm{d}\ln(\phi^j(z,t))}{\mathrm{d}t}$$

and subtracting these two equations yields

$$\frac{\mathrm{d}}{\mathrm{d}t}\ln\frac{f_i^j(t)\phi_i^j(z,t)}{f_i^k(z,t)\phi_i^k(z,t)} = \frac{\mathrm{d}}{\mathrm{d}t}\ln\frac{\phi^j(z,t)}{\phi^k(z,t)}.$$

Integrating both sides over t yields

$$\ln\frac{f_i^j(t)\phi_i^j(z,t)}{f_i^k(t)\phi_i^k(z,t)} = \ln\frac{\phi^j(z,t)}{\phi^k(z,t)} + c \tag{S1}$$

where

$$c = \ln\frac{f_i^j(0)\phi_i^j(z,0)\phi^k(z,0)}{f_i^k(0)\phi_i^k(z,0)\phi^j(z,0)}.$$

Hence,

$$\frac{f_i^j(t)\phi_i^j(z,t)}{f_i^k(t)\phi_i^k(z,t)} = C\frac{\phi^j(z,t)}{\phi^k(z,t)}$$

where

$$C = e^c = \frac{f_i^j(0)\phi_i^j(z,0)\phi^k(z,0)}{f_i^k(0)\phi_i^k(z,0)\phi^j(z,0)}.$$

Therefore, if

$$\frac{f_i^j(0)\phi_i^j(z,0)}{f_i^k(0)\phi_i^k(z,0)} = \frac{\phi^j(z,0)}{\phi^k(z,0)}$$

initially holds, then

$$\frac{f_i^j(t)\phi_i^j(z,t)}{f_i^k(t)\phi_i^k(z,t)} = \frac{\phi^j(z,t)}{\phi^k(z,t)}$$

holds for $t \geq 0$. This justifies equality (A.4).

S2 Projection on RV space: quasi-equilibrium approach

The goal of this appendix is to show how some results and arguments derived in Lion (2018) for unimodal distributions can be extended to multimodal distributions under the oligomorphic approximation by working at the morph level. Let us define $\mathbf{u}_i$ the vector with elements $f_i^k f^k / f_i$, $\mathbf{U}_i = \mathrm{diag}(\mathbf{u}_i)$, $\mathbf{C}_i$ the matrix with elements $\underset{\phi_i^j}{\mathrm{Cov}}\left(z, r^{kj}(z)\right)$, and $\mathbf{d}_i$ the vector of morph-specific scaled phenotypic differentiation (with elements $d_i^k = (\bar{z}_i^k - \bar{z}_i)/\sigma_i$ where $\sigma_i = \sqrt{V_i}$ is the standard deviation of the distribution of morph i). We can then write equation (C.1) as

$$\frac{\mathrm{d}\bar{z}_i}{\mathrm{d}t} = \mathbf{1}^\top \mathbf{C}_i \mathbf{u}_i + \sigma_i \mathbf{1}^\top \overline{\mathbf{R}}_i \mathbf{U}_i \mathbf{d}_i \tag{S2}$$

which has the same form as equation (15) in Lion (2018), but is morph-specific. Similarly, the dynamics of $\mathbf{d}_i$ can be put in the form:

$$\frac{\mathrm{d}(\sigma_i \mathbf{d}_i)}{\mathrm{d}t} = \mathbf{B}_i \mathbf{C}_i \mathbf{u}_i + \mathbf{A}_i (\sigma_i \mathbf{d}_i) \tag{S3}$$

which has the same form as equation (A2) in Lion (2018). Hence, if we assume, as in Lion (2018), that the unimodal morph distributions are tightly clustered around the mean (which is the crux of the oligomorphic approximation), we can follow the same approach as in that paper, and derive a quasi-equilibrium approximation for $\mathbf{d}_i$. This eventually yields:

$$\frac{\mathrm{d}\bar{z}_i}{\mathrm{d}t} \approx \mathbf{v}_i^\top \mathbf{S_i} \mathbf{\Omega}_i \mathbf{u}_i + O(\varepsilon^4) \tag{S4}$$

where $\mathbf{v}_i^\top$ and $\mathbf{u}_i$ are calculated as the left and right eigenvectors of $\mathbf{R}_i$ associated to eigenvalue 0, keeping only the $O(1)$ terms, $\mathbf{\Omega}_i = \mathrm{diag}(V_i^1 \dots V_i^K)$ and the matrix $\mathbf{S}_i$ has elements $\partial r^{kj}/\partial z$ evaluated at $z = \bar{z}_i^j$. To leading order, we can replace $\bar{z}_i^j$ and V_i^j by $\bar{z}_i$ and V_i (because both $\bar{z}_i^j - \bar{z}_i = O(\varepsilon^2)$ and $V_i^j - V_i = O(\varepsilon^4)$ on the slow time scale, as shown in Online Appendix S3) to obtain equation (19) in the main text. Doing so only contributes an $O(\varepsilon^4)$ error term.

Finally, a similar reasoning can be applied to the dynamics of variance, and we conjecture that the dynamics of all moments of the distribution $\phi_i(z,t)$ can be approximated by those of $\widetilde{\phi}_i(z,t)$ for small ε.

S3 Separation of time scales

In this appendix, we first show that the phenotypic differentiations $\bar{z}_i^k - \widetilde{z}_i$ converge to zero on the fast time scale, so that we can assume $\bar{z}_i^k - \widetilde{z}_i = O(\varepsilon^2)$ on the fast time scale. We then use a perturbation expansion approach to prove the separation of time scales between class densities and morph frequencies on the one hand, and morph means on the other hand. The arguments for the dynamics of variance are similar.

S3.1 Dynamics of phenotypic differentiation on the fast time scale

Let us introduce the deviations $D_k = \bar{z}_i^k - \widetilde{z}_i$, which measure the difference between the mean trait in class k and the RV-weighted mean trait $\widetilde{z}_i = \sum_k c_i^k \bar{z}_i^k$. We then have

$$\frac{\mathrm{d}\bar{z}_i^k}{\mathrm{d}t} = \sum_j \frac{u_i^j}{u_i^k} r^{kj}(\bar{z}_i^j)(\bar{z}_i^j - \bar{z}_i^k) + \sum_j \frac{u_i^j}{u_i^k} V_i^j \left.\frac{\partial r^{kj}}{\partial z}\right|_{z=\bar{z}_i^j} + O(\varepsilon^4)$$

$$\frac{\mathrm{d}\widetilde{z}_i}{\mathrm{d}t} = \sum_j u_i^j V_i^j \sum_k v_i^k \left.\frac{\partial r^{kj}}{\partial z}\right|_{z=\bar{z}_i^j} u_i^j + O(\varepsilon^4)$$

Subtracting the two equations and keeping only $O(1)$ terms yields

$$\begin{aligned}\frac{\mathrm{d}D_k}{\mathrm{d}t} &= \sum_j \frac{u_i^j}{u_i^k} r^{kj}(\bar{z}_i^j)(\bar{z}_i^j - \bar{z}_i^k) + O(\varepsilon^2) \\ &= \sum_j \frac{u_i^j}{u_i^k} r^{kj}(\bar{z}_i^j) D_j - D_k \sum_j \frac{u_i^j}{u_i^k} r^{kj}(\bar{z}_i^j) + O(\varepsilon^2)\end{aligned}$$

Writing the differentiation as the perturbation expansion $D_k = D_k^{(0)} + \varepsilon D_k^{(1)} + \ldots$, it follows that the zeroth-order term satisfies

$$\frac{\mathrm{d}\mathbf{D}^{(0)}}{\mathrm{d}t} = \mathbf{Q}\mathbf{D}^0$$

where the matrix $\mathbf{Q}$ has the following elements

$$k \neq j \quad q_{kj} = \frac{u_i^j}{u_i^k} r^{kj}(\bar{z}_i^j)$$

$$q_{kk} = -\sum_{j \neq k} \frac{u_i^j}{u_i^k} r^{kj}(\bar{z}_i^j)$$

Because $\sum_k c_i^k D_k = 0$ by definition, the system is overdetermined, but we can remove one redundant equation and write the dynamics of $\mathbf{D}_* = \begin{pmatrix} D_1 & \ldots & D_{K-1} \end{pmatrix}$. This gives

$$\frac{\mathrm{d}\mathbf{D}_*^{(0)}}{\mathrm{d}t} = \mathbf{Q}_* \mathbf{D}_*^{(0)}$$

where the matrix $\mathbf{Q}_*$ is a $(K-1)\times(K-1)$ matrix obtained from $\mathbf{Q}$ by expressing D_K as a function of the elements of $\mathbf{D}_*$ (Lion, 2018). If we assume for convenience that the phenotypic differentiation does not blow up and the system of class densities, morph frequencies and phenotypic differentiations reaches an equilibrium in the limit $\varepsilon \to 0$, and $\mathbf{Q}_*$ is invertible at this equilibrium, then we can characterise the equilibrium as $\mathbf{D}^{(0)} = \mathbf{0}$. Note that the same reasoning allows us to show that $\mathbf{D}^{(1)} = 0$, and therefore

$$\bar{z}_i^k - \widetilde{z}_i = \varepsilon^2 D_k^{(2)} = O(\varepsilon^2) \tag{S5}$$

This justifies that we can replace $\bar{z}_i^k$ by $\widetilde{z}_i$ on the slow time scale (i.e. after relaxation of the fast dynamics). Note that the argument above implicity requires that the classes must not be isolated, otherwise the transition rates r^{kj} are all zero for $j \neq k$, and there is no homogeneisation of the morph means on the fast time scale.

For the variance dynamics, plugging (S5) into equation (15) shows that the leading-order term of the dynamics of the variance differentiation $V_i^k - \widetilde{V}_i$ is

$$\frac{\mathrm{d}(V_i^k - \widetilde{V}_i)}{\mathrm{d}t} = \sum_j \frac{u_i^j}{u_i^k} r^{kj}(\bar{z}_i^j)(V_i^j - V_i^k) + O(\varepsilon^4)$$

which has the same form as the dynamics of $\mathbf{D}^{(0)}$ and therefore the same argument shows that

$$\bar{V}_i^k - \widetilde{V}_i = O(\varepsilon^4). \tag{S6}$$

S3.2 Two-class case

For the two-class case, we can use milder assumptions. Let $D_i(t) = \bar{z}_i^A(t) - \bar{z}_i^B(t)$ and $L_i(t) = D_i(t)^2$. Then, if we simply assume that $r^{AB}(z) > 0$ and $r^{BA}(z) > 0$ for any z (which will be realistic for many ODE ecological models), we have in our $O(1)$ system

$$\frac{dL_i(t)}{dt} = 2D_i(t)\frac{dD_i(t)}{dt} = -2\left(\frac{n_i^B(t)}{n_i^A(t)} r^{AB}(\bar{z}_i^B(t)) + \frac{n_i^A(t)}{n_i^B(t)} r^{BA}(\bar{z}_i^A(t))\right) D_i(t)^2 \leq 0,$$

where the equality holds only when $D_i = 0$. Therefore $L_i(t) = D(t)_i^2 \to 0$.

S3.3 Separation of time scales: perturbation expansion

Here, we use a perturbation expansion to analyse the separation of time scales in the oligomorphic equations. The argument is valid for a given morph i, so for simplicity we drop the i subscript. We have for the dynamics of class densities

$$\frac{\mathrm{d}n^k}{\mathrm{d}t} = \sum_j r^{kj}(\bar{z}^j)n^j + O(\varepsilon^2) \tag{S7}$$

and for the dynamics of class means

$$\frac{\mathrm{d}\bar{z}^k}{\mathrm{d}t} = \sum_j \frac{u^j}{u^k} r^{kj}(\bar{z}^j, \mathbf{n})(\bar{z}^j - \bar{z}^k) + \sum_j V^j \frac{u^j}{u^k} \left.\frac{\partial r^{kj}(z, \mathbf{n})}{\partial z}\right|_{z=\bar{z}^j} + O(\varepsilon^4) \tag{S8}$$

It is clear that the leading-order term of equation (S7) is $O(1)$. But so is the leading-order term of equation (S8). However, we will see that after relaxation of the fast dynamics, equation (S8) is $O(\varepsilon^2)$.

To show this, we use the following perturbation expansion:

$$n^k = n^k_{(0)} + \varepsilon n^k_{(1)} + \varepsilon^2 n^k_{(2)} + \dots$$
$$\bar{z}^k = \bar{z}^k_{(0)} + \varepsilon z^k_{(1)} + \varepsilon^2 \bar{z}^k_{(2)} + \dots$$

We first solve the system for the zeroth-order terms:

$$\frac{\mathrm{d}\bar{z}^k_{(0)}}{\mathrm{d}t} = \sum_j \frac{u^j}{u^k} r^{kj}\left(\bar{z}^j_{(0)}, \mathbf{n}_{(0)}\right)\left(\bar{z}^j_{(0)} - \bar{z}^k_{(0)}\right)$$

This system is obtained by Taylor-expanding equation (S8) and keeping only $O(1)$ terms. These dynamics tend to homogeneise the values of the mean traits, so (as we've just shown above) we have at equilibrium

$$\bar{z}^j_{(0)} - \bar{z}^k_{(0)} = 0 \qquad \text{for all } j, k \tag{S9}$$

We can use this quasi-equilibrium result to obtain the following system for the dynamics of $\mathbf{z}k_{(1)}$

$$\frac{\mathrm{d}\bar{z}^k_{(1)}}{\mathrm{d}t} = \sum_j \frac{u^j}{u^k} r^{kj}\left(\bar{z}^j_{(0)}, \mathbf{n}_{(0)}\right)\left(\bar{z}^j_{(1)} - \bar{z}^k_{(1)}\right)$$

This system is obtained by Taylor-expanding equation (S8) and keeping only $O(\varepsilon)$ terms. Again, this yields at equilibrium

$$\bar{z}^j_{(1)} - \bar{z}^k_{(1)} = 0 \qquad \text{for all } j, k \tag{S10}$$

In particular, this means that

$$\bar{z}^k - \widetilde{z} = \sum_j c^j(\bar{z}^k - \bar{z}^j) = \varepsilon^2 \sum_j c^j(\bar{z}^k_{(2)} - \bar{z}^j_{(2)})$$

and therefore

$$\bar{z}^k = \widetilde{z} + O(\varepsilon^2).$$

We then use the quasi-equilibrium solutions of (S9) and (S10) to derive the dynamics of the $O(\varepsilon^2)$ terms as

$$\frac{\mathrm{d}\bar{z}^k_{(2)}}{\mathrm{d}t} = \sum_j \frac{u^j}{u^k} r^{kj}(\bar{z}^j_{(0)}, \mathbf{n}_{(0)})(\bar{z}^j_{(2)} - \bar{z}^k_{(2)}) + \sum_j W^j \frac{u^j}{u^k} \frac{\partial r^{kj}}{\partial z}(\bar{z}^j_{(0)}, \mathbf{n}_{(0)}) + O(\varepsilon^2) \tag{S11}$$

where $V^j = \epsilon^2 W^j$.

Thus, after relaxation of the fast dynamics, we have

$$\frac{\mathrm{d}\bar{z}^k}{\mathrm{d}t} = \varepsilon^2 \frac{\mathrm{d}\bar{z}^k_{(2)}}{\mathrm{d}t} + O(\varepsilon^4)$$

where $\frac{\mathrm{d}\bar{z}^k_{(2)}}{\mathrm{d}t}$ can be calculated using equation (S11).

Note that equation (S11) depends on the zeroth-order terms of densities $\mathbf{n}$, but actually, if we use $\mathbf{n}$ instead of $\mathbf{n}_{(0)}$ in equation (S11), the error we make will be absorbed in the $O(\varepsilon^2)$ remainder. Similarly, it is possible to replace $\bar{z}^j_{(0)}$ by $\bar{z}^j$ or $\widetilde{z}$ in the arguments of r^{kj}, so we can also write more simply

$$\frac{\mathrm{d}\bar{z}^k_{(2)}}{\mathrm{d}t} = \sum_j \frac{u^j}{u^k} r^{kj}(\bar{z}^j, \mathbf{n})(\bar{z}^j_{(2)} - \bar{z}^k_{(2)}) + \sum_j W^j \frac{u^j}{u^k} \frac{\partial r^{kj}}{\partial z}(\bar{z}^j, \mathbf{n}) + O(\varepsilon^2) \tag{S12}$$

In words, this analysis indicates that, starting from distinct morph means in each class, the morph means first change quickly to become clustered around an average value (i.e. $\bar{z}^k_i \approx \widetilde{z}_i$) then change more slowly along the slow manifold. On this manifold, the densities are well approximated by the quasi-equilibrium solution of $\mathbf{n}_{(0)}$.

Note that the dynamics of the RV-weighted mean trait, $\widetilde{z}$, is $O(\varepsilon^2)$ from the start, which is why it is much easier to use it to describe the slow dynamics.

S4 Quasi-equilibrium approximation of reproductive values in two-class models

In two class models, the equations $\bar{\mathbf{R}}_i \mathbf{u}_i = \mathbf{0}$ and $\mathbf{v}_i \bar{\mathbf{R}}_i = \mathbf{0}$ can be rewritten as

$$r^{AA}u^A + r^{AB}u^B = 0 \tag{S13a}$$

$$r^{BA}u^A + r^{BB}u^B = 0 \tag{S13b}$$

$$v^A r^{AA} + v^B r^{BA} = 0 \tag{S13c}$$

$$v^A r^{AB} + v^B r^{BB} = 0 \tag{S13d}$$

where for simplificity we remove the dependency on the morph (i.e. we write u_i^k as u^k, v_i^k as v^k, and $r^{kj}(\bar{z}_i^j)$ as r^{kj}.

Using equation (S13c), we can rewrite the normalisation conditions $u^A v^A + u^B v^B = 1$ as

$$-u^A \frac{r^{BA}}{r^{AA}} v^B + u^B v^B = 1 \tag{S14}$$

which leads to

$$v^B = \frac{r^{AA}}{r^{AA}u^B - r^{BA}u^A} \tag{S15}$$

and, using equation (S13a), which can be rewritten as $r^{AA} = -r^{AB}u^B/u^A$, we obtain finally

$$v^B = \frac{r^{AB}u^B}{r^{AB}(u^B)^2 + r^{BA}(u^A)^2} \tag{S16}$$

A similar equation can be obtained for v^A (we just need to swap the A and B superscripts) and multiplying by u^B yields

$$c^B = \frac{r^{AB}(u^B)^2}{r^{AB}(u^B)^2 + r^{BA}(u^A)^2} = 1 - c^A \tag{S17}$$

which is equation (D.3).

S5 Oligomorphic dynamics in a two-class migration-selection model

We use equation (22) in the main text to derive the oligomorphic dynamics when there are only two classes and when the only transitions between distinct classes correspond to migra-

tion and are independent of the focal trait under consideration. That is, we have:

$$r^{AB}(z) = m_{AB}$$
$$r^{BA}(z) = m_{BA}$$

With this simplifying assumption, we obtain the following equations, which will be used to analyse our three Examples:

$$\frac{\mathrm{d}}{\mathrm{d}t}\begin{pmatrix} n^A \\ n^B \end{pmatrix} = \begin{pmatrix} \sum_i f_i^A r^{AA}(\bar{z}_i^A) & m_{AB} \\ m_{BA} & \sum_i f_i^B r^{BB}(\bar{z}_i^B) \end{pmatrix}\begin{pmatrix} n^A \\ n^B \end{pmatrix} + O(\varepsilon^2) \tag{S18a}$$

$$\frac{\mathrm{d}f_i^A}{\mathrm{d}t} = f_i^A\left[r^{AA}(\bar{z}_i^A) - \sum_\ell f_\ell^A r^{AA}(\bar{z}_\ell^A)\right] + \frac{n^B}{n^A}m_{AB}\left[f_i^B - f_i^A\right] + O(\varepsilon^2) \tag{S18b}$$

$$\frac{\mathrm{d}f_i^B}{\mathrm{d}t} = f_i^B\left[r^{BB}(\bar{z}_i^B) - \sum_\ell f_\ell^B r^{BB}(\bar{z}_\ell^B)\right] + \frac{n^A}{n^B}m_{BA}\left[f_i^A - f_i^B\right] + O(\varepsilon^2) \tag{S18c}$$

$$\frac{\mathrm{d}\bar{z}_i^A}{\mathrm{d}t} = V_i^A\left.\frac{\partial r^{AA}}{\partial z}\right|_{z=\bar{z}_i^A} + \frac{f_i^B n^B}{f_i^A n^A}m_{AB}(\bar{z}_i^B - \bar{z}_i^A) + O(\varepsilon^4) \tag{S18d}$$

$$\frac{\mathrm{d}\bar{z}_i^B}{\mathrm{d}t} = V_i^B\left.\frac{\partial r^{BB}}{\partial z}\right|_{z=\bar{z}_i^B} + \frac{f_i^A n^A}{f_i^B n^B}m_{BA}(\bar{z}_i^A - \bar{z}_i^B) + O(\varepsilon^4) \tag{S18e}$$

$$\frac{\mathrm{d}V_i^A}{\mathrm{d}t} = \frac{1}{2}\left[Q_i^A - (V_i^A)^2\right]\left.\frac{\partial^2 r^{AA}}{\partial z^2}\right|_{z=\bar{z}_i^A} + \frac{f_i^B n^B}{f_i^A n^A}m_{AB}\left[V_i^B - V_i^A + (\bar{z}_i^B - \bar{z}_i^A)^2\right] + O(\varepsilon^5) \tag{S18f}$$

$$\frac{\mathrm{d}V_i^B}{\mathrm{d}t} = \frac{1}{2}\left[Q_i^B - (V_i^B)^2\right]\left.\frac{\partial^2 r^{BB}}{\partial z^2}\right|_{z=\bar{z}_i^B} + \frac{f_i^A n^A}{f_i^B n^B}m_{BA}\left[V_i^A - V_i^B + (\bar{z}_i^A - \bar{z}_i^B)^2\right] + O(\varepsilon^5) \tag{S18g}$$

S6 Example 1: A two-habitat local adaptation model

In this appendix, we carry out an explicit analysis of a specific two-habitat model to revisit the results of Débarre et al. (2013) (see also Mirrahimi and Gandon (2020); Ronce and Kirkpatrick (2001)). As in that paper and in Online Appendix S5, we consider a population of individuals distributed over two habitats, A and B, coupled by migration. Each habitat is characterised by a habitat-specific optimum (θ_A and θ_B, respectively). The transition rates between classes

are then

$$r^{AA}(z) = b - n^A - g(z-\theta_A)^2 - m_{BA} \tag{S19a}$$

$$r^{AB}(z) = m_{AB} \tag{S19b}$$

$$r^{BA}(z) = m_{BA} \tag{S19c}$$

$$r^{BB}(z) = b - n^B - g(z-\theta_B)^2 - m_{AB} \tag{S19d}$$

where b is the fecundity rate and g is the fecundity cost. We use quadratic cost functions for simplicity, so that the cost is minimal at the habitat's optimum. Also, in contrast to Débarre et al. (2013), we consider asymmetric migration rates, with m_{jk} the migration rate from habitat k to habitat j (see also Mirrahimi and Gandon (2020)). Note that we assume migration rates do not depend on the focal trait, which will lead to simplifications as the partial derivatives of $r^{kj}(z)$ will vanish for $j \neq k$.

Note that this model can be simply obtained from the competition model in Online Appendix S7 by assuming $a(\cdot) = 1$.

S6.1 Oligomorphic approximation

To derive our oligormorphic approximation for this model, we combine equations (S18) with the following relationships

$$r^{kk}(\bar{z}_i^k) = b - w_k(\bar{z}_i^k) - m_k - n^k \tag{S20a}$$

$$\left.\frac{\partial r^{kk}}{\partial z}\right|_{z=\bar{z}_i^k} = -w_k'(\bar{z}_i^k) \tag{S20b}$$

$$\left.\frac{\partial^2 r^{kk}}{\partial z^2}\right|_{z=\bar{z}_i^k} = -w_k''(\bar{z}_i^k) \tag{S20c}$$

where $w_A(z) = g(z-\theta_A)^2$, $w_B(z) = g(z-\theta_B)^2$, $m_A = m_{BA}$ and $m_B = m_{AB}$.

Reproductive values. The resulting system can be numerically solved, but we can get some further simplifications using reproductive values. Using equation (D.3), we see that class reproductive values satisfy at quasi-equilibrium

$$c_i^B = \frac{m_{AB}(f_i^B f^B)^2}{m_{AB}(f_i^B f^B)^2 + m_{BA}(f_i^A f^A)^2} = 1 - c_i^A \tag{S21}$$

where the morph and class frequencies are calculated using the $O(1)$ terms of equations (S18a)-(S18c).

Morph means. Using equations (S4) and (C.2), it is straightforward to derive the following equation for the dynamics of the morph mean, $\bar{z}_i$, and the RV-weighted morph mean $\widetilde{z}_i$. We obtain

$$\frac{\mathrm{d}\bar{z}_i}{\mathrm{d}t} = \frac{\mathrm{d}\widetilde{z}_i}{\mathrm{d}t} = c_i^A V_i^A \left.\frac{\partial r^{AA}}{\partial z}\right|_{z=\bar{z}_i^A} + c_i^B V_i^B \left.\frac{\partial r^{BB}}{\partial z}\right|_{z=\bar{z}_i^B} + O(\varepsilon^4) \tag{S22}$$

If we only want to keep $O(\varepsilon^2)$ terms, it is sufficient to replace V_i^A and V_i^B by V_i, the morph variance, and $\bar{z}_i^A$ and $\bar{z}_i^B$ by the morph mean $\bar{z}_i$ (Online Appendix S3). We then obtain for our model:

$$\frac{\mathrm{d}\bar{z}_i}{\mathrm{d}t} = -V_i\left[c_i^A w'_A(\bar{z}_i) + c_i^B w'_B(\bar{z}_i)\right] + O(\varepsilon^4) \approx -2gV_i\left[\bar{z}_i - c_i^A\theta_A - c_i^B\theta_B\right] \tag{S23}$$

An explicit derivation of equation (S22) can also be obtained by calculating the dynamics of $\bar{z}_i^B - \bar{z}_i^A$ which is simply obtained by substracting equations (S18d)-(S18e). Then, treating this phenotypic differentiation as a fast variable (Lion (2018); Online Sections S2; S3), we can set the right-hand side of the resulting equation to zero, and solve for $\bar{z}_i^B - \bar{z}_i^A$. This yields the following quasi-equilibrium approximation

$$\bar{z}_i^B - \bar{z}_i^A \approx \frac{f_i^A f^A f_i^B f^B}{m_{AB}(f_i^B f^B)^2 + m_{BA}(f_i^A f^A)^2}\left(V_i^B \left.\frac{\partial r^{BB}}{\partial z}\right|_{z=\bar{z}_i^B} - V_i^A \left.\frac{\partial r^{AA}}{\partial z}\right|_{z=\bar{z}_i^A}\right) \tag{S24}$$

which can be written using equation (S21) as

$$\bar{z}_i^B - \bar{z}_i^A \approx \sqrt{\frac{c_i^A c_i^B}{m_{AB}m_{BA}}}\left(V_i^B \left.\frac{\partial r^{BB}}{\partial z}\right|_{z=\bar{z}_i^B} - V_i^A \left.\frac{\partial r^{AA}}{\partial z}\right|_{z=\bar{z}_i^A}\right) \tag{S25}$$

Plugging the resulting expression into equations (S18d) and (S18e) yields

$$\frac{\mathrm{d}\bar{z}_i^A}{\mathrm{d}t} = \frac{\mathrm{d}\bar{z}_i^B}{\mathrm{d}t} = c_i^A V_i^A \left.\frac{\partial r^{AA}}{\partial z}\right|_{z=\bar{z}_i^A} + c_i^B V_i^B \left.\frac{\partial r^{BB}}{\partial z}\right|_{z=\bar{z}_i^B} + O(\varepsilon^4) \tag{S26}$$

which entails, assuming that the morph and class frequencies are calculated on their quasi-equilibrium manifold,

$$\frac{\mathrm{d}\bar{z}_i}{\mathrm{d}t} = \frac{\mathrm{d}\widetilde{z}_i}{\mathrm{d}t} = \frac{\mathrm{d}\bar{z}_i^A}{\mathrm{d}t} = \frac{\mathrm{d}\bar{z}_i^B}{\mathrm{d}t}$$

Equation (S25) shows that $\bar{z}_i^B - \bar{z}_i^A = O(\varepsilon^2)$, so that $\bar{z}_i^A = \bar{z}_i^B = \bar{z}_i + O(\varepsilon^2)$. This is consistent with the general argument in Online Appendix S3 and justifies that we can replace the class-specific morph means by the morph mean in equation (S22). We then obtain equation (29)

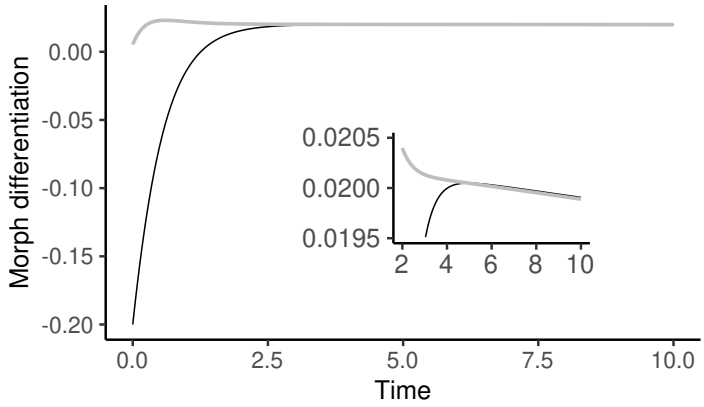

Figure S1: **Illustration of the relaxation to RV space in a two-class model.** The simulation is the same as in figure 2 and figure S3B, to which the reader is referred for additional details. The morph differentiation $\bar{z}_{B,1} - \bar{z}_{A,1}$ (black) is shown to converge towards the value predicted by the quasi-equilibrium approximation (S24) (grey line). The inset shows a close-up of the dynamics.

in the main text. Figure S1 shows that the differentiation between morph means $\bar{z}_{B,1} - \bar{z}_{A,1}$ quickly converges to a small value which is well predicted by the quasi-equilibrium approximation.

Morph variances. Similarly, we can derive the dynamics of the difference in morph variances from equations (S18f)-(S18g). With Gaussian closure approximation (such that $Q_i^k = 3(V_i^k)^2$) and using equation (S21), we obtain after some rearrangements the following quasi-equilibrium approximation:

$$V_i^B - V_i^A \approx \sqrt{\frac{c_i^A c_i^B}{m_{AB} m_{BA}}} \left[(V_i^B)^2 \left.\frac{\partial^2 r^{BB}}{\partial z^2}\right|_{z=\bar{z}_i^B} - (V_i^A)^2 \left.\frac{\partial^2 r^{AA}}{\partial z^2}\right|_{z=\bar{z}_i^A} \right] - (c_i^B - c_i^A)(\bar{z}_i^B - \bar{z}_i^A)^2 \quad \text{(S27)}$$

Plugging this into equations (S18f) and (S18g) yields, again after some rearrangements

$$\frac{\mathrm{d}V_i^A}{\mathrm{d}t} = \frac{\mathrm{d}V_i^B}{\mathrm{d}t} = c_i^A (V_i^A)^2 \left.\frac{\partial^2 r^{AA}}{\partial z^2}\right|_{z=\bar{z}_i^A} + c_i B (V_i^B)^2 \left.\frac{\partial^2 r^{BB}}{\partial z^2}\right|_{z=\bar{z}_i^B} + 2\sqrt{c_i^A c_i^B m_{AB} m_{BA}} (\bar{z}_i^B - \bar{z}_i^A)^2 \quad \text{(S28)}$$

and using equation (S25) finally yields

$$\begin{aligned}\frac{\mathrm{d}V_i^A}{\mathrm{d}t} = \frac{\mathrm{d}V_i^B}{\mathrm{d}t} =& c_i^A (V_i^A)^2 \left.\frac{\partial^2 r^{AA}}{\partial z^2}\right|_{z=\bar{z}_i^A} + c_i^B (V_i^B)^2 \left.\frac{\partial^2 r^{BB}}{\partial z^2}\right|_{z=\bar{z}_i^B} \\ &+ 2\frac{\left(c_i^A c_i^B\right)^{3/2}}{\sqrt{m_{AB} m_{BA}}} \left(V_i^B \left.\frac{\partial r^{BB}}{\partial z}\right|_{z=\bar{z}_i^B} - V_i^A \left.\frac{\partial r^{AA}}{\partial z}\right|_{z=\bar{z}_i^A} \right)^2 \end{aligned} \tag{S29}$$

which again implies

$$\frac{\mathrm{d}V_i}{\mathrm{d}t} = \frac{\mathrm{d}\widetilde{V}_i}{\mathrm{d}t} = \frac{\mathrm{d}V_i^A}{\mathrm{d}t} = \frac{\mathrm{d}V_i^B}{\mathrm{d}t}$$

Another route to this result is to start with the dynamics of the RV-weighted variance, given by equation (21). This gives for our model

$$\begin{aligned}\frac{\mathrm{d}\widetilde{V}_i}{\mathrm{d}t} \approx& c_i^A (V_i^A)^2 \left.\frac{\partial^2 r^{AA}}{\partial z^2}\right|_{z=\bar{z}_i^A} + c_i^B (V_i^B)^2 \left.\frac{\partial^2 r^{BB}}{\partial z^2}\right|_{z=\bar{z}_i^B} \\ &+ 2c_i^A (\bar{z}_i^A - \widetilde{z}_i) V_i^A \left.\frac{\partial r^{AA}}{\partial z}\right|_{z=\bar{z}_i^A} + 2c_i^B (\bar{z}_i^B - \widetilde{z}_i) V_i^B \left.\frac{\partial r^{AA}}{\partial z}\right|_{z=\bar{z}_i^B} \end{aligned} \tag{S30}$$

(recall that $v_i^k u_i^k = c_i^k$). Noting that $\bar{z}_i^A - \widetilde{z}_i = c_i^B(\bar{z}_i^A - \bar{z}_i^B)$ and $\bar{z}_i^B - \widetilde{z}_i = c_i^A(\bar{z}_i^B - \bar{z}_i^A)$, and using equation (S25) finally yields

$$\begin{aligned}\frac{\mathrm{d}\widetilde{V}_i}{\mathrm{d}t} =& c_i^A (V_i^A)^2 \left.\frac{\partial^2 r^{AA}}{\partial z^2}\right|_{z=\bar{z}_i^A} + c_i^B (V_i^B)^2 \left.\frac{\partial^2 r^{BB}}{\partial z^2}\right|_{z=\bar{z}_i^B} \\ &+ 2\frac{\left(c_i^A c_i^B\right)^{3/2}}{\sqrt{m_{AB} m_{BA}}} \left(V_i^B \left.\frac{\partial r^{BB}}{\partial z}\right|_{z=\bar{z}_i^B} - V_i^A \left.\frac{\partial r^{AA}}{\partial z}\right|_{z=\bar{z}_i^A} \right)^2 \end{aligned} \tag{S31}$$

From equation (S27) we see that $V_i^B - V_i^A = O(\varepsilon^4)$, so that $V_i^A = V_i^B = \widetilde{V}_i + O(\varepsilon^4)$. The errors made by approximating the class-specific variances by $\widetilde{V}_i$ in equation (S31) will therefore be of higher-order than the leading-order terms.

S6.2 Quadratic functions

For the model with quadratic functions, equations (S22) and (S31) simplify to

$$\frac{\mathrm{d}\bar{z}_i}{\mathrm{d}t} = -2gV_i \left[\bar{z}_i - c_i^A \theta_A - c_i^B \theta_B\right] \tag{S32}$$

$$\frac{\mathrm{d}V_i}{\mathrm{d}t} = -2gV_i^2 \left[1 - \frac{4g}{\sqrt{m_{AB} m_{BA}}} \left(c_i^A c_i^B\right)^{3/2} (\theta_B - \theta_A)^2\right] \tag{S33}$$

Equation (S32) shows that at equilibrium morph means are equal to the reproductive-value weighted average of habitat optima, $c_i^A \theta_A + c_i^B \theta_B$. As shown in Sasaki and Dieckmann (2011),

the corresponding equilibra are all evolutionarily stable if and only if $\mathrm{d}V_i/\mathrm{d}t < 0$ for all morphs, which is equivalent to

$$\frac{\sqrt{m_{AB}m_{BA}}}{4g} > \left(c_i^A c_i^B\right)^{3/2} \tag{S34}$$

where we have set $\theta_A = 0 = 1 - \theta_B$ without loss of generality.

S6.3 Solutions

We consider that the population is composed of two morphs (1 and 2). From equations (S18b) and (S18c), together with equations (S19), we can thus write the dynamics of the frequencies of morph 1 in habitats A and B as follows:

$$0 = (f_1^A(1-f_1^A)g(\bar{z}_1 - \bar{z}_2)(\bar{z}_1 + \bar{z}_2) + m_{AB}\frac{f^B}{f^A}(f_1^B - f_1^A) \tag{S35}$$

$$0 = (f_1^B(1-f_1^B)g(\bar{z}_1 - \bar{z}_2)(\bar{z}_1 + \bar{z}_2 - 2) + m_{BA}\frac{f^A}{f^B}(f_1^A - f_1^B) \tag{S36}$$

Multiplying the first equation by $f^A/(m_{AB}f^B)$ and the second by $f^B/(m_{BA}f^A)$, then taking the sum, gives

$$0 = g(\bar{z}_1 - \bar{z}_2)\left[\frac{f^A f_1^A(1-f_1^A)}{m_{AB}f^B}(\bar{z}_1 + \bar{z}_2) + \frac{f^B f_1^B(1-f_1^B)}{m_{BA}f^A}(\bar{z}_1 + \bar{z}_2 - 2)\right] \tag{S37}$$

This is satisfied either if $\bar{z}_1 = \bar{z}_2$ which corresponds to a single-morph equilibrium, or if the term between brackets is zero, which leads to a dimorphic equilibrium

Dimorphic equilibrium. We start with the dimorphic case, which is simpler to analyse. Setting the term between brackets in equation (S37) to zero yields

$$\frac{f_1^B(1-f_2^B)}{f_1^A(1-f_1^A)} = \frac{\bar{z}_1 + \bar{z}_2}{2 - \bar{z}_1 - \bar{z}_2}\frac{m_{BA}}{m_{AB}}\left(\frac{f^A}{f^B}\right)^2 \tag{S38}$$

From the equilibrium of equation (S32), we have $\bar{z}_i = c_i^B$, and because $c_i^A = 1 - c_i^B$, we thus have $\bar{z}_i/(1-\bar{z}_i) = c_i^B/c_i^A$. From equation (S21), we then have

$$\bar{z}_i/(1-\bar{z}_i) = (m_{AB}/m_{BA})(f_i^B f^B/(f_i^A f^A))^2,$$

which we can use to simplify equation (S38) as

$$\frac{\bar{z}_1\bar{z}_2}{(1-\bar{z}_1)(1-\bar{z}_2)} = \left(\frac{\bar{z}_1 + \bar{z}_2}{2 - \bar{z}_1 - \bar{z}_2}\right)^2$$

which can be rearranged as

$$(\bar{z}_1 - \bar{z}_2)^2(1 - \bar{z}_1 - \bar{z}_2) = 0$$

Hence, because $\bar{z}_1 \neq \bar{z}_2$ for the dimorphic equilibrium, the morph means must satisfy $\bar{z}_1 + \bar{z}_2 = 1$. Plugging this condition into the dynamics of morph frequencies, then solving for f_1^A and f_1^B and calculating c_1^B yields

$$\bar{z}_1 = c_1^B = \frac{1}{2} - \frac{g(1-2\bar{z}_1)}{2\sqrt{4m_{AB}m_{BA} + g^2(1-2\bar{z}_1^2)}}$$

Solving for $\bar{z}_1$ finally yields, for $\sqrt{m_{AB}m_{BA}} < g/2$

$$\boxed{\bar{z}_1 = \frac{1}{2} - \frac{1}{2}\sqrt{1 - \frac{4m_{AB}m_{BA}}{g^2}} = 1 - \bar{z}_2} \tag{S39}$$

which, using equation (S33), is evolutionarily stable if $\sqrt{m_{AB}m_{BA}} < g/2$. Equation (S39) corresponds to the results of Mirrahimi and Gandon (2020) and, for the symmetric migration case, to those of Débarre et al. (2013).

Equation (S39) can be used to calculate the morph frequencies (see companion Mathematica notebook). In the same notebook, we also derive the following expressions for the equilibrium densities

$$n^A = b - m_{BA} + \frac{m_{AB}m_{BA}}{g}$$
$$n^B = b - m_{AB} + \frac{m_{AB}m_{BA}}{g}$$

For symmetric migration, we recover the results in Table 1 of Débarre et al. (2013).

Because the dimorphic equilibrium is characterised by the two morphs having different frequencies in the two habitats, the habitat-specific trait distributions are distinct. We can characterise these equilibrium distributions by calculating their moments (see companion notebook):

- the mean trait in habitats A and B (and the differentiation $D = \bar{z}^B - \bar{z}^A$)

$$\bar{z}^A = f_1^A\bar{z}_1 + (1 - f_1^A)\bar{z}_2 = \frac{m_{AB}f^B}{gf^A}$$
$$\bar{z}^B = f_1^B\bar{z}_1 + (1 - f_1^B)\bar{z}_2 = 1 - \frac{m_{BA}f^A}{gf^B}$$

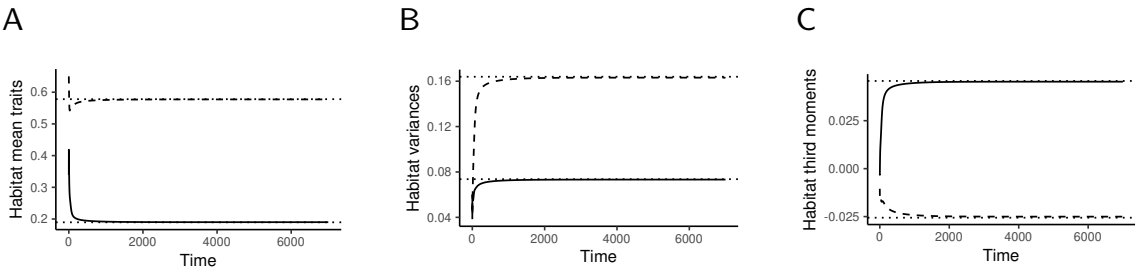

Figure S2: **Dynamics of habitat-specific moments**. The means (a), variances (b) and third moments (c) of the trait distributions in habitat A (solid lines) and B (dashed lines) and shown to converge to the values predicted by the analytical formulae (dotted horizontal lines). Parameters as in figure 3B in the main text.

- the global mean trait

$$\bar{z} = f^A \bar{z}^A + f^B \bar{z}^B = f^B + \frac{m_{AB} f^B - m_{BA} f^A}{g}$$

  where the first term is the mean of the two optima ($f^A \theta_A + f^B \theta_B = f^B$) and the second term is the deviation caused by the migration-selection balance. For symmetric migration, we have $\bar{z} = f^B = 1/2$.

- the variance in habitat A in the absence of mutation-selection balance (i.e. assuming $V_i^A = 0$ at equilibrium)

$$V^A = (\bar{z}_1 - \bar{z}^A)^2 f_1^A + (\bar{z}_2 - \bar{z}^B)^2 (1 - f_1^A) = m_{AB} \frac{f^A f^B g - m_{AB} (f^B)^2 - m_{BA} (f^A)^2}{(f^A g)^2}$$

- the third moment in habitat A in the absence of mutation-selection balance (i.e. assuming $V_i^A = 0$ at equilibrium), assuming the morph distribution is not skewed (e.g. $T_i^A = 0$)

$$T^A = (\bar{z}_1 - \bar{z}^A)^3 f_1^A + (\bar{z}_2 - \bar{z}^B)^3 (1 - f_1^A) = \frac{f^A g - 2 f^B m_{AB}}{f^A g} V^A$$

Note that, for symmetric migration, we recover the results of Débarre et al. (2013) (column 2 in their Table 1). In figure S2, the dynamics of the moments of the trait distributions in habitats A and B are presented and compared with the analytical predictions.

Local adaptation. At the bimodal equilibrium, the two morphs have different frequencies in the two habitats and therefore the habitat-specific distributions are distinct (figure 3B). As

shown by Débarre et al. (2013), local adaptation in this model is proportional to the level of habitat differentiation in mean traits, which can be calculated as

$$D = \bar{z}^B - \bar{z}^A = (f_1^B - f_1^A)(c_1^B - c_2^B). \tag{S40}$$

This shows that, at equilibrium, local adaptation depends (1) on the difference in morph frequencies between the two habitats, and (2) on the difference between the class reproductive values of the two morphs. Using the above results, habitat differentiation can be calculated as:

$$D^* = 1 - \frac{1}{g}\left(\frac{f^B}{f^A}m_{AB} + \frac{f^A}{f^B}m_{BA}\right) \tag{S41}$$

which simplifies to $D^* = 1 - 2m/g$ for symmetric migration, as found in Débarre et al. (2013). Higher migration thus leads to lower local adaptation.

Single-morph equilibria. In the single-morph case, we have only one morph with frequencies $f_1^A = f_1^B = 1$. The equilibrium densities and morph mean can be calculated from the following system of equations:

$$\begin{aligned}
\frac{\mathrm{d}n^A}{\mathrm{d}t} &= \left(b - n^A - g\bar{z}_1^2 - m_{BA}\right)n^A + m_{AB}n^B = 0 \\
\frac{\mathrm{d}n^B}{\mathrm{d}t} &= \left(b - n^B - g(\bar{z}_1 - 1)^2 - m_{AB}\right)n^B + m_{BA}n^A = 0 \\
\bar{z}_1 &= \frac{m_{AB}(n^B)^2}{m_{AB}(n^B)^2 + m_{BA}(n^A)^2}
\end{aligned}$$

where the latter equation simply states that the mean trait is equal to the class reproductive value c_1^B.

The system can only be fully solved numerically, except for symmetric migration where at least one solution ($\bar{z}_1 = 1/2$ and $n^A = n^B = b - g/4$) can be analytically calculated. Depending on the region of parameter space (and in particular the values of the migration rates) there is typically either one or three solutions of the system.

Note that, in the limit where $m_{AB} = m_{BA} = m$, we have $v_1^A = v_1^B = 1$ and therefore $\bar{z}_1 = c_1^B = 1/2$. The "symmetric monomorphic" singularity found by Débarre et al. (2013) thus corresponds to the case where both habitats have equal reproductive values. As found by Débarre et al. (2013), this solution is evolutionarily stable if $m > g/2$, which can be checked using condition (S33).

Bistability. For some parameters values, the system can exhibit several evolutionary attractors (i.e. convergent and evolutionarily stable points, Geritz et al. (1998)), notably the dimorphic equilibrium and one or two single-morph equilibria. The endpoint of the eco-evolutionary dynamics is then determined by the initial conditions. This bistability is illustrated in figure S3 for a specific example, and the full bifurcation diagrams of the model for $m_{AB} = 0.8$ are shown in figures S4. Note however that, as already found by Débarre et al. (2013), the basin of attraction of the unimodal equilibrium is relatively narrow so that a little mutation is sufficient to push the dynamics towards the bimodal equilibrium. This explains why the simulations of the full model (the black dots in figures S4A and S4B) typically converge towards the bimodal equilibrium when it exists. Thus, while the oligomorphic analysis predicts bistability when $m < m_c$, with some initial conditions leading to unimodal equilibrium distributions, a global stability analysis shows that the bimodal distribution is the more robust evolutionary outcome (Mirrahimi and Gandon, 2020).

S6.4 Accuracy of the RV projection

How accurate is it to replace the equations (22) the projection of RV space ? Figure S4 shows that the quantitative match is very good, except in a small region of parameter space between $m_{AB} = 0.8$ and $m_{BA} = 1$, where the RV projection does not accurately predicts the single-morph solution. This corresponds to a point where migration is close to symmetric and the single-morph solution actually becomes a repellor. Thus the dynamics converge towards a point where selection is disruptive but a dimorphism cannot persist. As shown in figure S5B, this causes the build-up of subtantial differentiation between the morph means in habitats A and B, at which point the morph-centred reproductive-value-weighted oligomorphic approximation breaks down.

S6.5 Effect of mutation

In this section, we give additional results for the analysis of the effect of mutation variance shown in figure 4B. In these simulations, we assume $V_M^A = V_M^B = V_M$. Figure S6 shows how the mutational variance affects the equilibrium trait distributions in habitat A (top panel)

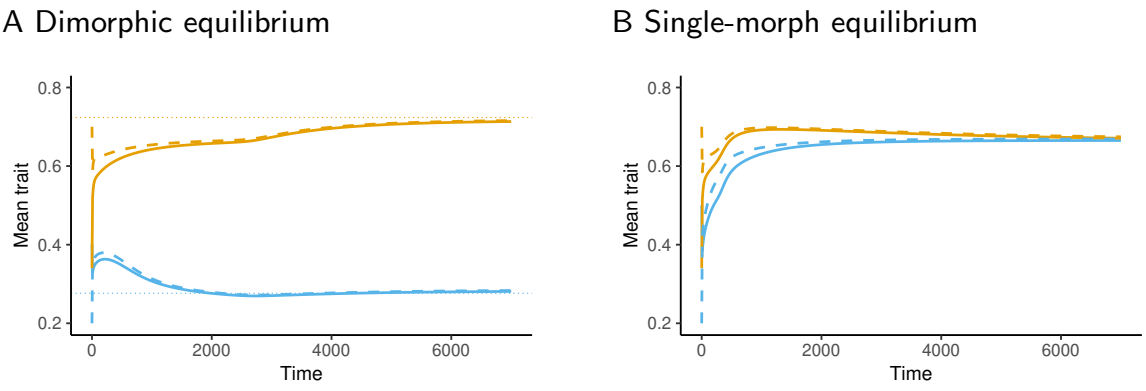

Figure S3: **Illustration of the bistable dynamics of the model for sufficiently low values of the geometric mean of the migration rate**, $m = \sqrt{m_{AB} m_{BA}}$. The dynamics of the mean trait of morph 1 (blue) and 2 (black) in habitat A (solid lines) and B (dashed lines) are shown, either leading to a polymorphic equilibrium (left panel) or to a monomorphic equilibrium (panel b). The only difference between the two simulations is the initial trait value of the first morph in habitat A, which is $x_1^A(0) = 0.4$ in panel (a), and $x_1^A(0) = 0.5$ in panel (b). Other initial conditions: $n_A(0) = n_B(0) = 1$, $f_i^k(0) = 1/2$ (for $i = 1, 2$ and $k = A, B$), $x_2^A(0) = 0.34$, $x_1^B(0) = 0.2$, $x_2^B(0) = 0.7$, $V_1^A(0) = V_1^B(0) = 0.002$, $V_2^A(0) = V_2^B(0) = 0.001$. Parameters: $m_{AB} = 0.8$, $m_{BA} = 1$, $g = 2$, $b = 1$.

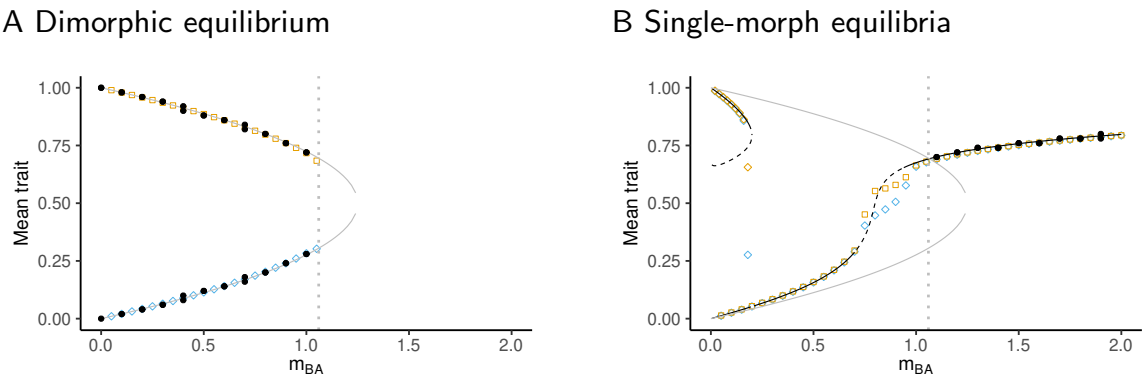

Figure S4: **Bistability.** Figures (a) and (b) give the bifurcation diagrams for the mean traits. Open shapes give the predictions of a two-morph oligomorphic approximation for the dimorphic (circles, panel b) and single-morph (diamonds, panel c) solutions, for both morphs 1 (blue) and 2 (orange). The gray lines represent the analytical expressions $1/2 \pm \sqrt{1-4m^2/g^2}/2$, which are shown on both panels (b) and (c) for convenience. The results of the full model, without the oligomorphic approximation, are presented using black dots. On panel (b), the black lines give the predictions of the oligomorphic approximation (solid lines represent evolutionarily stable, and dashed lines evolutionarily unstable solutions). In all panels, the vertical dotted line represents the value $m_{BA} \approx 1.06$ at which the dimorphic equilibrium loses its demographic stability and one of the two morphs goes extinct. Parameter values: $b = 1$, $g = 2$, $m_{AB} = 0.8$, $V_M = 10^{-6}$.

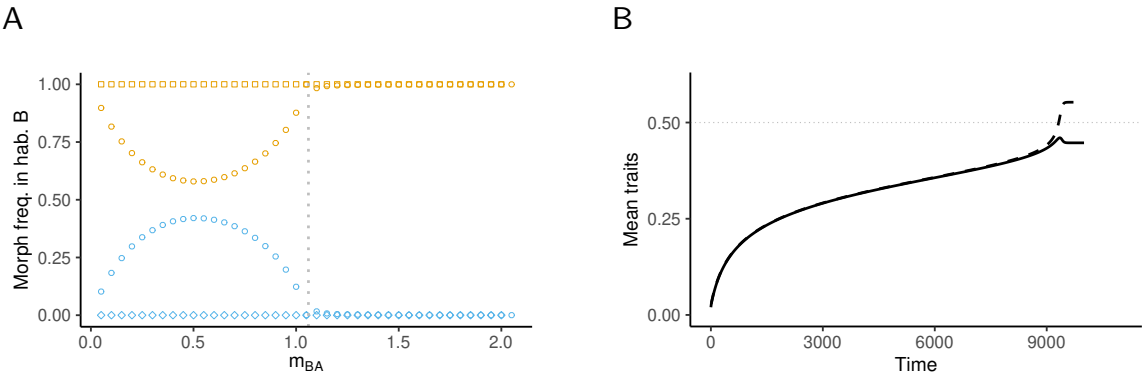

Figure S5: This figure gives some additional results which are helpful to better understand figure S4 Panel (a) gives the corresponding equilibrium values of the frequencies of morphs 1 (blue) and 2 (orange) for the single-morph (diamonds) and two-morph (circles) equilibria. Panel (b) represents the dynamics of the mean trait in habitat A (solid line) and B (dashed line) predicted by the single-morph oligomorphic approximation for $m_{AB} = m_{BA} = 0.8$. In all panels, the vertical dotted line represents the value $m_{BA} \approx 1.06$ at which the dimorphic equilibrium loses its demographic stability and one of the two morphs goes extinct. Parameters as in figure 3.

and B (middle panel), and the morph frequencies (bottom panel). There is a sharp change in behaviour around $V_M \approx 10^{-3}$, which corresponds to the oligomorphic approximation breaking down when the morph variances become too large and the morph distributions collide: we then shift from a dimorphism with two distinct morphs (distinct frequencies of morph 1 and 2 in each habitat, but the morph means are the same in each habitat $\bar{z}_i^A = \bar{z}_i^B = \bar{z}_i$) to a case where one morph suddenly goes extinct, but this morph has a distinct mean in each habitat (i.e. $\bar{z}_1^A \neq \bar{z}_1^B$). However, the simulations of the full model do not predict this pattern, but rather than the model always converges towards a bimodal distributions with two peaks, albeit with slightly wider variances when V_M is larger. Since the oligomorphic approximation relies on morph variances (i.e. the width of the peaks) being small enough, this is an expected behaviour of our approach. Nonetheless, the oligomorphic approximation remains accurate for relatively large mutational variance, approximately of the same order as the morph variance.

When the mutational variances are different in habitats A and B, we have the following expression for the morph variance at the mutation-selection equilibrium:

$$V_i^* = \sqrt{\frac{c_i^A V_M^A + c_i^B V_M^B}{2g\left[1 - \frac{4g}{m}(c_i^A c_i^B)^{3/2}\right]}} \tag{S42}$$

with $m = \sqrt{m_{AB} m_{BA}}$. Using the expression (S39) and the fact that $\bar{z}_i = c_i^B = 1 - c_i^A$ at evolutionary equilibrium, it is straightforward to obtain a closed analytical expression:

$$V_1^* = \sqrt{\frac{\left(\frac{1}{2} + \frac{1}{2}\sqrt{1 - \frac{4m^2}{g^2}}\right) V_M^A + \left(\frac{1}{2} - \frac{1}{2}\sqrt{1 - \frac{4m^2}{g^2}}\right) V_M^B}{2g\left[1 - \frac{4m^2}{g^2}\right]}} \tag{S43}$$

and

$$V_2^* = \sqrt{\frac{\left(\frac{1}{2} - \frac{1}{2}\sqrt{1 - \frac{4m^2}{g^2}}\right) V_M^A + \left(\frac{1}{2} + \frac{1}{2}\sqrt{1 - \frac{4m^2}{g^2}}\right) V_M^B}{2g\left[1 - \frac{4m^2}{g^2}\right]}} \tag{S44}$$

These expressions correspond to the horizontal dotted lines in the top panel of figure 4A.

S7 Example 2: A two-habitat resource-competition model

In this appendix, we consider a population of individuals distributed over two habitats, A and B, coupled by migration. We extend the resource-competition model analysed in Sasaki

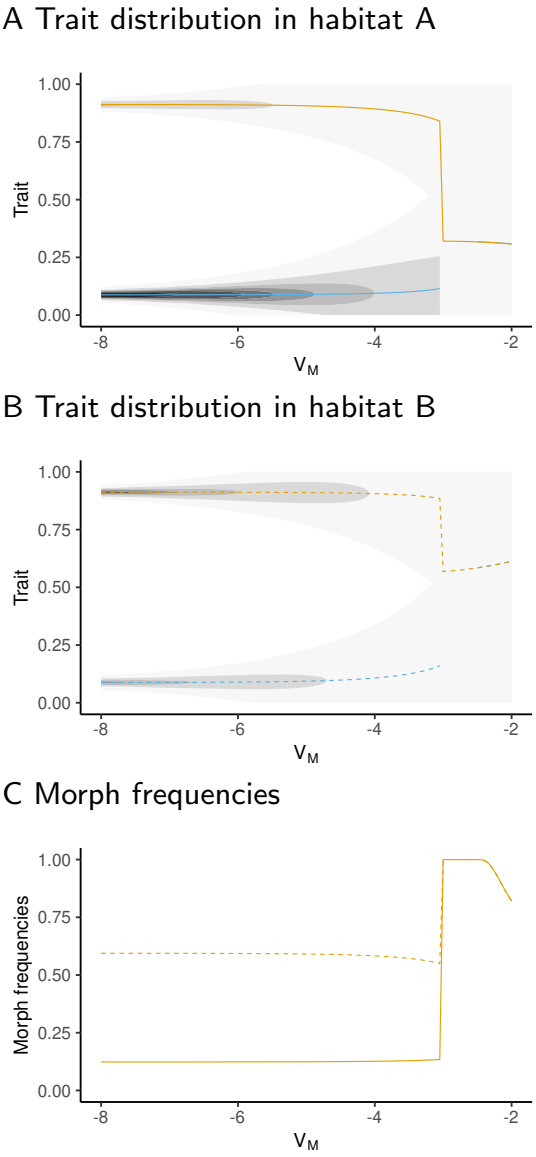

Figure S6: **Effect of mutation.** The density distribution in habitats A (panel (a)) and B (panel (b)), and the frequencies of morph 2 in each habitat (panel (c); A: solid, B: dashed) are shown as a function of the mutational variance V_M (log scale). When V_M increases, the variance of the distributions increases. There is a threshold at $V_M \approx 10^{-3}$ above which the oligomorphic approximation breaks down.

and Dieckmann (2011) to model migration across classes, and class-specific trait-mediated competition for resources. The transition rates between classes are then

$$\begin{aligned} r^{AA}(z) &= b - n^A \int a(z-y)\phi^A(y,t)\mathrm{d}y - g(z-\theta_A)^2 - m_{BA} \\ r^{AB}(z) &= m_{AB} \\ r^{BA}(z) &= m_{BA} \\ r^{BB}(z) &= b - n^B \int a(z-y)\phi^B(y,t)\mathrm{d}y - g(z-\theta_B)^2 - m_{AB} \end{aligned}$$

where b is the fecundity rate and g is a fecundity cost. We use quadratic cost functions for simplicity, so that the cost is minimal at the habitat optima θ_A and θ_B. The function $a(z-y)$ is the competition kernel, which gives the intensity of competition experienced by individuals with trait z when they interact with individuals with trait y. We assume that the kernel is a symmetric function of the trait difference, so that $a(z-y) = a(y-z)$, and furthermore we assume, as in Sasaki and Dieckmann (2011), that $a(0) = 1$ and $a'(0) = 0$. In the case where only one habitat is present, this corresponds to the model studied by Sasaki and Dieckmann (2011).

Oligomorphic dynamics. The dynamics of the densities, frequencies, means and variances are given by system (S18) We use the oligomorphic approximation to calculate the derivatives of the rates $r^{AA}(z)$ and $r^{BB}(z)$ for the specific case of Example 2. As in Sasaki and Dieckmann (2011), we first Taylor-expand the competition kernel around $y = \bar{z}_\ell^j$ to obtain

$$a(z-y) = a(z-\bar{z}_\ell^j) + a'(z-\bar{z}_\ell^j)(y-\bar{z}_\ell^j) + \frac{1}{2}a''(z-\bar{z}_\ell^j)(y-\bar{z}_\ell^j)^2 + O(\varepsilon^3)$$

Multiplying by $f_\ell^j\phi_\ell^j(y,t)$ and summing over ℓ yields

$$\begin{aligned} a(z-y)\phi^j(y,t) = &\sum_\ell f_\ell^j a(z-\bar{z}_\ell^j)\phi_\ell^j(y,t) + \sum_\ell f_\ell^j a'(z-\bar{z}_\ell^j)(y-\bar{z}_\ell^j)\phi_\ell^j(y,t) \\ &+ \frac{1}{2}\sum_\ell f_\ell^j a''(z-\bar{z}_\ell^j)(y-\bar{z}_\ell^j)^2\phi_\ell^j(y,t) + O(\varepsilon^3) \end{aligned}$$

Integrating over y, we obtain:

$$\int a(z-y)\phi^j(y,t)\mathrm{d}y = \sum_\ell f_\ell^j a(z-\bar{z}_\ell^j) + \frac{1}{2}\sum_\ell f_\ell^j V_\ell^j a''(z-\bar{z}_\ell^j) + O(\varepsilon^3)$$

We can then write the vital rates as

$$r^{AA}(z) = b - n^A \sum_\ell f_\ell^A a(z - \bar{z}_\ell^A) - g(z - \theta_A)^2 - m_{BA} + O(\varepsilon^2)$$
$$r^{BB}(z) = b - n^B \sum f_\ell^B a(z - \bar{z}_\ell^B) - g(z - \theta_B)^2 - m_{AB} + O(\varepsilon^2)$$

and the partial derivatives:

$$\left.\frac{\partial r^{AA}}{\partial z}\right|_{z=\bar{z}_i^A} = -n^A \sum_\ell f_\ell^A a'(\bar{z}_i^A - \bar{z}_\ell^A) - 2g(\bar{z}_i^A - \theta_A) + O(\varepsilon^2)$$
$$\left.\frac{\partial^2 r^{AA}}{\partial z^2}\right|_{z=\bar{z}_i^A} = -n^B \sum_\ell f_\ell^A a''(\bar{z}_i^B - \bar{z}_\ell^B) - 2g + O(\varepsilon^2)$$

with similar expressions for the partial derivatives in habitat B. We can then use these expressions in equations (S18) to obtain the general oligomorphic approximation of the resource competition model. This is how the numerical simulations in figure 5 in the main text (plain and dashed lines) were performed.

Projection on RV space. We can also plug these expressions into equations (S22) and (S31) to obtain the projection on RV space:

$$\frac{\mathrm{d}\bar{z}_i}{\mathrm{d}t} = V_i \left[-2g(\bar{z}_i - c_i^B) - \sum_\ell (c_i^A n^A f_\ell^A + c_i^B n^B f_\ell^B) a'(\bar{z}_i - \bar{z}_\ell) \right] \tag{S45}$$

$$\frac{\mathrm{d}V_i}{\mathrm{d}t} = -V_i^2 \left\{ 2g + \sum_\ell (c_i^A n^A f_\ell^A + c_i^B n^B f_\ell^B) a''(\bar{z}_i - \bar{z}_\ell) - 2\frac{(c_i^A c_i^B)^{3/2}}{m} \left[2g - \sum_\ell (n^A f_\ell^A + n^B f_\ell^B) a'(\bar{z}_i - \bar{z}_\ell) \right]^2 \right\} \tag{S46}$$

With only one morph and a Gaussian kernel (i.e. $a(x) = \kappa \exp(-x^2/(2\omega^2))$) such that $a'(0) = 0$ and $a''(0) = -\kappa/\omega^2$), this yields

$$\frac{\mathrm{d}\bar{z}_1}{\mathrm{d}t} = -2gV_1 \left[\bar{z}_1 - c_1^B \right]$$
$$\frac{\mathrm{d}V_1}{\mathrm{d}t} = -2gV_1^2 \left[1 - \frac{\kappa}{\omega^2}(c_1^A n^A + c_1^B n^B) - \frac{4g}{m}(c_1^A c_1^B)^{3/2} \right]$$

with $m = \sqrt{m_{AB} m_{BA}}$,

$$c_1^B = \frac{m_{AB}(f^B)^2}{m_{BA}(f^A)^2 + m_{AB}(f^B)^2} = \frac{m_{AB}(n^B)^2}{m_{BA}(n^A)^2 + m_{AB}(n^B)^2}$$

(this directly follows from equation (D.3)) and

$$\frac{\mathrm{d}n^A}{\mathrm{d}t} = \left(b - n^A a(0) - g(\bar{z}_1)^2 - m_{BA}\right) n^A + m_{AB} n^B$$
$$\frac{\mathrm{d}n^B}{\mathrm{d}t} = \left(b - n^B a(0) - g(\bar{z}_1 - 1)^2 - m_{AB}\right) n^B + m_{BA} n^A$$

With two morphs and a Gaussian kernel, we have

$$\frac{\mathrm{d}\bar{z}_1}{\mathrm{d}t} = -2gV_1 \left[\bar{z}_1 - c_1^B - \frac{e_1}{2g} a'(\bar{z}_1 - \bar{z}_2)\right]$$
$$\frac{\mathrm{d}\bar{z}_2}{\mathrm{d}t} = -2gV_2 \left[\bar{z}_2 - c_2^B - \frac{e_2}{2g} a'(\bar{z}_2 - \bar{z}_1)\right]$$

with

$$c_i^B = \frac{m_{AB}(f_i^B f^B)^2}{m_{BA}(f_i^A f^A)^2 + m_{AB}(f_i^B f^B)^2}$$

and

$$e_1 = c_1^A n^A f_2^A + c_1^B n^B f_2^B,$$
$$e_2 = c_2^A n^A f_1^A + c_2^B n^B f_2^B,$$

together with the dynamics of morph variances (equation (S46)) and of $n^k(t)$, $f_i^k(t)$ (equations (S18a)-(S18c) with $\bar{z}_i^A = \bar{z}_i^B = \bar{z}_i$). The dotted lines in figure 5 show the results of the numerical integration of this two-morph system.

S8 Example 3: A two-habitat resource-consumer model

We now consider a resource-consumer model where the fitness function of individuals with trait z in habitat k are given by

$$\rho_k(z) = b(z)\frac{S^k}{1 + \tau S^k} - d(z) - n^k \tag{S47}$$

where S^k is the density of resource in habitat k, $b(z)$ is the fecundity rate, $d(z)$ the mortality rate, and τ the handling time (that is we assume a type-II functional response). We assume a trade-off between fecundity and survival, and in particular, for our simulations, we will use

$$b(z) = b_0 \frac{z}{1+z} \qquad \text{and} \qquad d(z) = 1 + z$$

We have the following transition rates

$$r^{AA}(z) = \rho_A(z) - m_{BA}$$

$$r^{AB}(z) = m_{AB}$$

$$r^{BA}(z) = m_{BA}$$

$$r^{BB}(z) = \rho_B(z) - m_{AB}$$

and the eco-evolutionary dynamics of the consumer population can be approximated using equations (S18), together with the following equations for the dynamics of the resources:

$$\frac{\mathrm{d}S^A}{\mathrm{d}t} = \theta\nu(1-\zeta S^A) - \delta S^A - S^A \sum_i \left(b(\bar{z}_i^A) n^A f_i^A + b(\bar{z}_i^B) n^B f_i^B \right) \tag{S48a}$$

$$\frac{\mathrm{d}S^B}{\mathrm{d}t} = \theta(1-\nu)(1-\zeta S^B) - \delta S^B - S^B \sum_i \left(b(\bar{z}_i^A) n^A f_i^A + b(\bar{z}_i^B) n^B f_i^B \right) \tag{S48b}$$

We therefore assume that the resource is produced in each habitat in a biased manner (first term on the right-hand sides), and decays at rate δ in both habitats (second term). The third term describes the depletion of resource due to the exploitation by the consumer, and is simply derived by a Taylor-expansion of

$$\int b(z) n^k \phi^k(z,t) \mathrm{d}z = n^k \sum_i \int b(z) \phi_i^k(z,t) f_i^k = n^k \sum_i f_i^k b(\bar{z}_i^k) + O(\varepsilon^2)$$

For this example, we are interested in the dynamics of the mean trait in a given habitat, that is across the different peaks of the multi-modal distribution. The mean trait in habitat A can be calculated as

$$\bar{z}^A = \sum_i f_i^A \bar{z}_i^A.$$

Differentiating this equation yields

$$\frac{\mathrm{d}\bar{z}^A}{\mathrm{d}t} = \sum_i \bar{z}_i^A \frac{\mathrm{d}f_i^A}{\mathrm{d}t} + \sum_i f_i^A \frac{\mathrm{d}\bar{z}_i^A}{\mathrm{d}t} \tag{S49}$$

The first term tells us how the mean trait in habitat A changes when the height of the peaks change (e.g. the frequencies). This describes fast dynamics. The second term tells us how the mean trait in habitat A changes when the positions of the peaks change (e.g. the morph means). This describes slow dynamics. To simplify the second term, we use the projection on RV space and write

$$\frac{\mathrm{d}\bar{z}_i^A}{\mathrm{d}t} \approx \frac{\mathrm{d}\bar{z}_i}{\mathrm{d}t} = V_i \left(c_i^A \rho'_A(\bar{z}_i) + c_i^B \rho'_B(\bar{z}_i) \right) \tag{S50}$$

To simplify the first term we assume that we have only two morphs. Then $f_1^A = 1 - f_2^A$ and we obtain

$$\sum_i \bar{z}_i^A \frac{\mathrm{d}f_i^A}{\mathrm{d}t} = (\bar{z}_1^A - \bar{z}_2^A)\frac{\mathrm{d}f_1^A}{\mathrm{d}t} \tag{S51}$$

and use equation (S18b) to obtain

$$\frac{\mathrm{d}f_1^A}{\mathrm{d}t} = f_1^A(1-f_1^A)\Delta\rho + \frac{f^B}{f^A} m_{AB}(f_1^B - f_1^A) \tag{S52}$$

where $\Delta\rho_A = \rho_A(\bar{z}_1) - \rho_A(\bar{z}_2)$ is the average difference in growth rates between the two morphs.

Using the approximation $\bar{z}_1^A - \bar{z}_2^A \approx \bar{z}_1 - \bar{z}_2$ and inserting equations (S50) and (S52) into equation (S49) yields

$$\begin{aligned}\frac{\mathrm{d}\bar{z}^A}{\mathrm{d}t} = (\bar{z}_1 - \bar{z}_2)&\left[f_1^A(1-f_1^A)\Delta\rho_A + \frac{f^B}{f^A} m_{AB}(f_1^B - f_1^A)\right] \\ &+ \sum_i f_i^A V_i \left[c_i^A \rho'_A(\bar{z}_i) + c_i^B \rho'_B(\bar{z}_i)\right]\end{aligned}$$

which is equation (37) in the main text.

An interesting limit is when the population eventually becomes monomorphic (say morph 1 goes to fixation), in which case $f_1^A = f_1^B = 1$ and therefore the first line vanishes, and the dynamics of $\bar{z}^A$ collapse to:

$$\frac{\mathrm{d}\bar{z}^A}{\mathrm{d}t} V_1 \left[c_1^A \rho'_A(\bar{z}_1) + c_1^B \rho'_B(\bar{z}_1)\right] \tag{S53}$$

and we have $\bar{z}^A = \bar{z}_1^A$. The term between brackets is the selection gradient one would obtain from an invasion analysis in a monomorphic population and allows us to calculate evolutionary singularities. In this model, with the trade-off functions we choose, we obtain the following implicit relationship:

$$\bar{z}^{A,*} = \sqrt{b_0\left(c_1^A \frac{S^A}{1+\tau S^A} + c_1^B \frac{S^B}{1+\tau S^B}\right)} - 1 \tag{S54}$$

Additional figures. In the main text, we discuss a specific scenario and we provide here two additional figures. Figure S7 presents the same simulation results as in figure 6 in the main text but presents the dynamics of the morph frequencies and morph means, instead of the class-level means and variances. Figure S8 presents the same scenario as in figure 6 in the main text, but starting from two morphs that have very similar trait values, so that the overall standing variation in the population is small.

Parameter values. For this scenario, we use the following parameter values: $\theta = 8$, $\zeta = 0.25$, $\nu = 0.2$, $d = 1$, $\delta = 0.8$, $b_0 = 7$, $\tau = 0.5$, $V_M = 10^{-5}$, $m_{AB} = 0.2$, $m_{BA} = 0.4$. See the companion notebook for more details on the initial conditions.

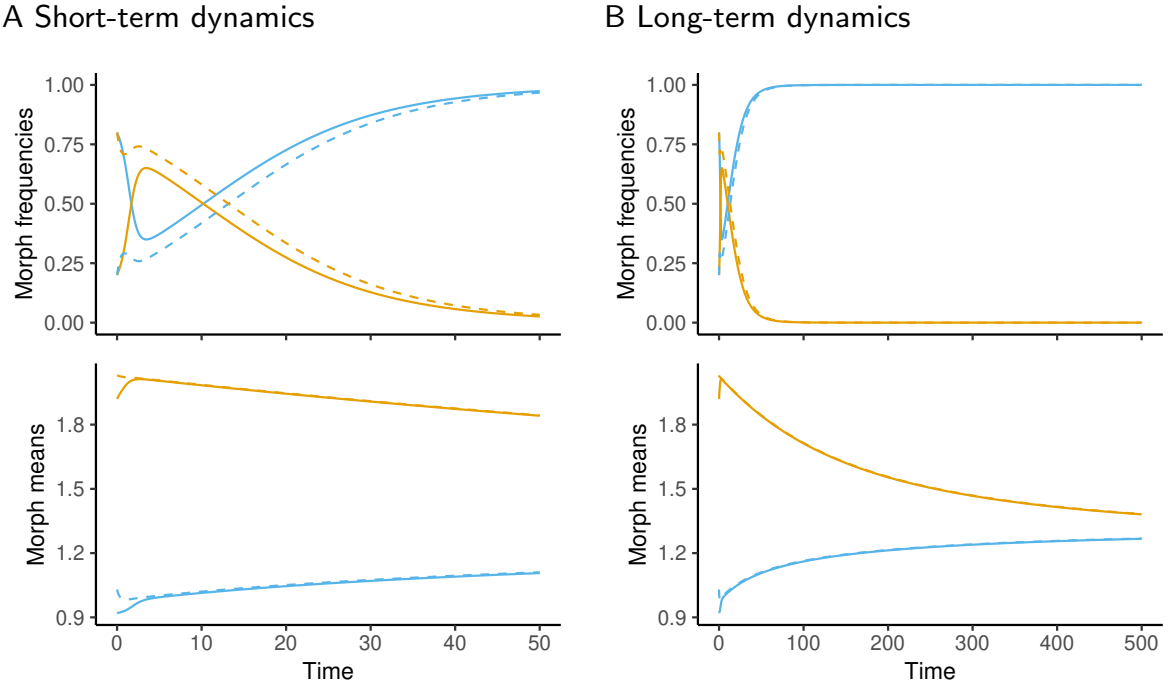

Figure S7: Dynamics of morph frequencies (top panel) and morph means (bottom panel) in the simulations of figure 6 in the main text, for both short-term (a) and long-term (b) dynamics.

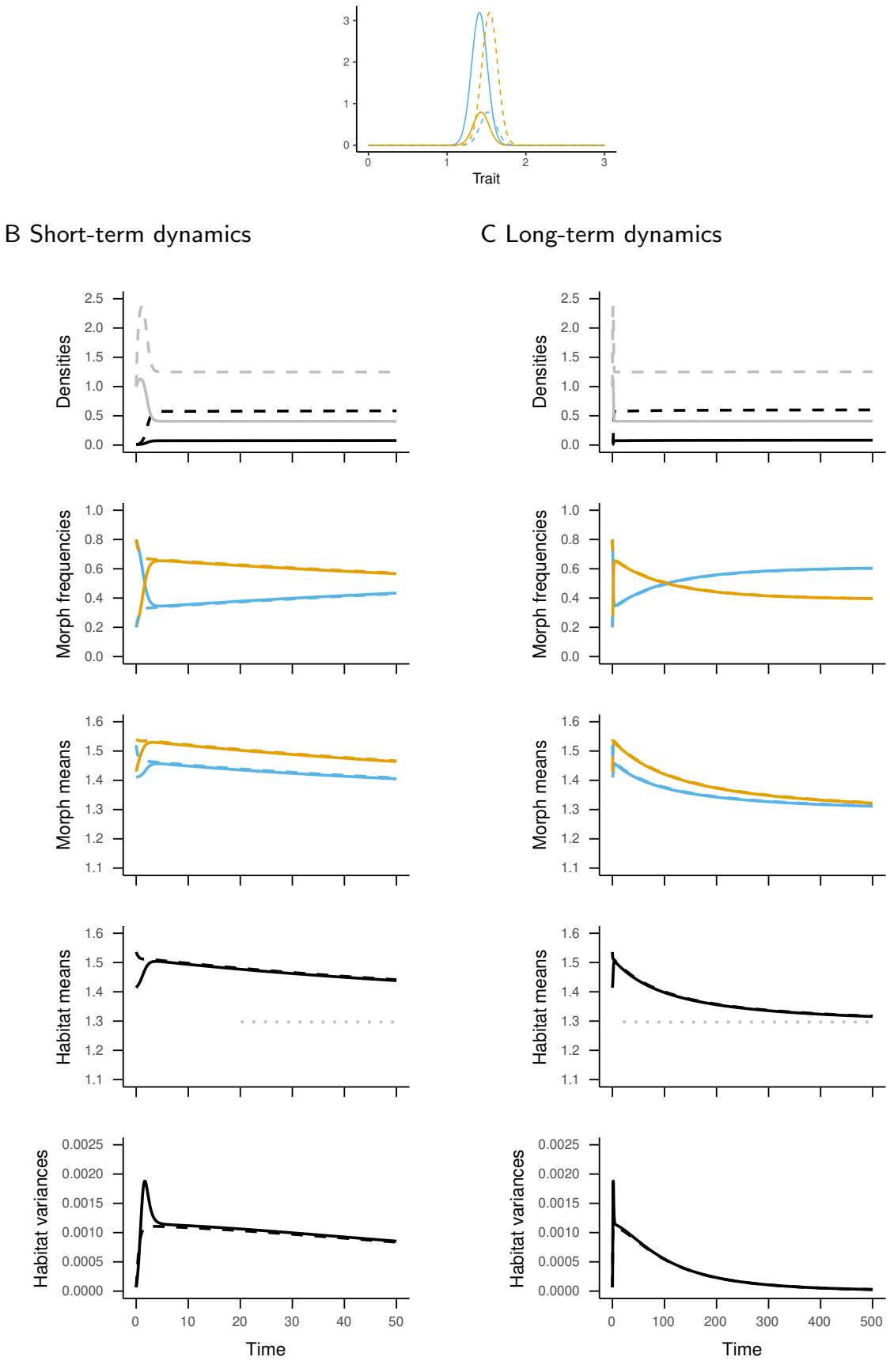

Figure S8: Same as in figure 6 in the main text, but when the two morphs are very close.

References

Débarre, F., O. Ronce, and S. Gandon. 2013. Quantifying the effects of migration and mutation on adaptation and demography in spatially heterogeneous environments. J. evol. Biol. 26:1185–1202.

Geritz, S. A. H., E. Kisdi, G. Meszéna, and J. A. J. Metz. 1998. Evolutionarily singular strategies and the adaptive growth and branching of the evolutionary tree. Evol. Ecol. 12:35–57.

Lion, S. 2018. From the Price equation to the selection gradient in class-structured populations: a quasi-equilibrium route. J. theor. Biol. 447C:178–189.

Mirrahimi, S., and S. Gandon. 2020. Evolution of specialization in heterogeneous environments: equilibrium between selection, mutation and migration. Genetics 214:479–491.

Ronce, O., and M. Kirkpatrick. 2001. When sources become sinks: migrational meltdown in heterogeneous habitats. Evolution 55:1520–1531.

Sasaki, A., and U. Dieckmann. 2011. Oligomorphic dynamics for analyzing the quantitative genetics of adaptive speciation. J. math. Biol. 63:601–35.